Singh, S., Mukherjee, P. K., Jain, A. K., Khanna, P. P., Saini, N. K. and Kumar, R. 2002. Source characterization and possible emplacement mechanism of collision-related Gangotri Leucogranite along Bhagirathi Valley, NW-Himalaya.
In: Singh, S. 2003. Granitiods of the Himalayan Collisional Belt. Journal of the Virtual Explorer, 11.

Source characterization and possible emplacement mechanism of collision-related Gangotri Leucogranite along Bhagirathi Valley, NW-Himalaya

SANDEEP SINGH[1], P. K. MUKHERJEE[2], A. K. JAIN[1], P. P. KHANNA[2], N.K. SAINI[2] AND RAJEEV KUMAR[1]

[1] Department of Earth Sciences, Indian Institute of Technology Roorkee, Roorkee – 247 667, India
[2] Wadia Institute of Himalayan Geology, 33 Gen. Mahadeo Singh Road, Ballupur, Dehradun – 248 001, India
email: sandpfes@iitr.ernet.in

Abstract: The Gangotri leucogranite is one of the largest bodies in the Higher Himalayan Leucogranite (HHL) belt. They occur as en-echelon lenses within the Pan-African S-type granitoid body. The possible source of proximal high-grade metasedimentary rocks and migmatites has yet to be established due to contrasting geochemistry. However, the observed geochemical linearity in binary variation diagrams and the sub-parallel nature of REE and spider-diagram patterns and other trace element data for the Pan-African body and tourmaline-bearing leucogranite suggest that the Pan-African body is the best potential source candidate. The separation of a small fraction of felsic melt from the source due to high viscosity is attributed to compactional or shearing stress during the syn-collisional event of Himalayan orogeny. The geochemical signatures also suggest that the leucogranites were produced by a lower degree of partial melting probably at shallower depth and low temperature.

Keywords: Himalayan granites, collisional magmatism, geochemistry, geochronology, Higher Himalayan Leucogranite belt

Introduction

The Himalayan orogenic belt contains various granitoids, which have been assigned ages ranging from Proterozoic to Late Cenozoic by earlier workers, mainly based on field relationships, nature of xenoliths, degree of metamorphism, petrographical similarities, structural trends, etc., prior to radiometric age dating (McMahon, 1884; Greisbach, 1893; Auden, 1935; Wadia, 1928, 1957; and others). Workers have also observed that most of the peaks with heights over 7,000 m are made up of gneiss, granite or crystalline rocks in the Higher Himalaya and beyond (Odell, 1983). The Himalayan granitoids can be broadly classified into two main types in relation to the Himalayan orogeny: (i) pre-collisional granite/gneiss and (ii) syn-to post-collisional leucogranite. Geochronological data, reported on a variety of granitoids and minerals using different radioactive systems, have constrained the age of emplacement, cooling and exhumation history (Pande, 1999; Jain et al., 2000; Hodges, 2000; Singh, 2001 and references therein). Age data from the granitoids of the Himalaya reveal distinct episodes of magmatic activity around 2100-1800 Ma, 1200-1000 Ma, 600-400 Ma, 100-50 Ma and 25-15Ma (Singh, 2001).

The Himalayan granitoids have varied geographical distribution along diverse stratigraphic and tectonic set up as linear belts parallel to the Himalayan orogen. Large granitoid bodies occur in almost all the tectonic units, except the Sub-Himalaya. On the basis of the geographical distribution, granitic plutons constitute five major belts in the Himalaya and adjoining Karakoram (Le Fort, 1988). From north to south, these belts include (Fig. 1 and 2) namely; Karakoram Batholith Complex, Trans-Himalayan Batholith, Northern Himalayan Granite Belt, Granitoids of the Higher Himalayan Crystallines (HHC) Belt, and Lesser Himalayan Granite Belt.

The Higher Himalayan Leucogranite (HHL), form the part of granitoids of the Higher Himalayan Crystallines (HHC), is of great interest to geologists working in orogenic belts and provides important information about the tectonic and metamorphic processes during orogenesis. Such leucogranites also occur in other regions of Western Europe, SE-Asia and Western United States, but their volume is relatively small. The Himalayan leucogranite, occurring as a belt, is probably the best exposed and among the most intensively studied granites so far. The High Himalayan Leucogranite (HHL) forms a discontinuous belt for about 1500 km from Pakistan to Bhutan (Fig. 2), having numerous intrusions of varying dimensions (Debon et al., 1986). These occur as sills laccoliths and are intruded either within the HHC or near its interface with the overlying unmetamorphosed to weakly metamorphosed Tethyan Sedimentary Zone (TSZ), where a major structural break of Miocene age

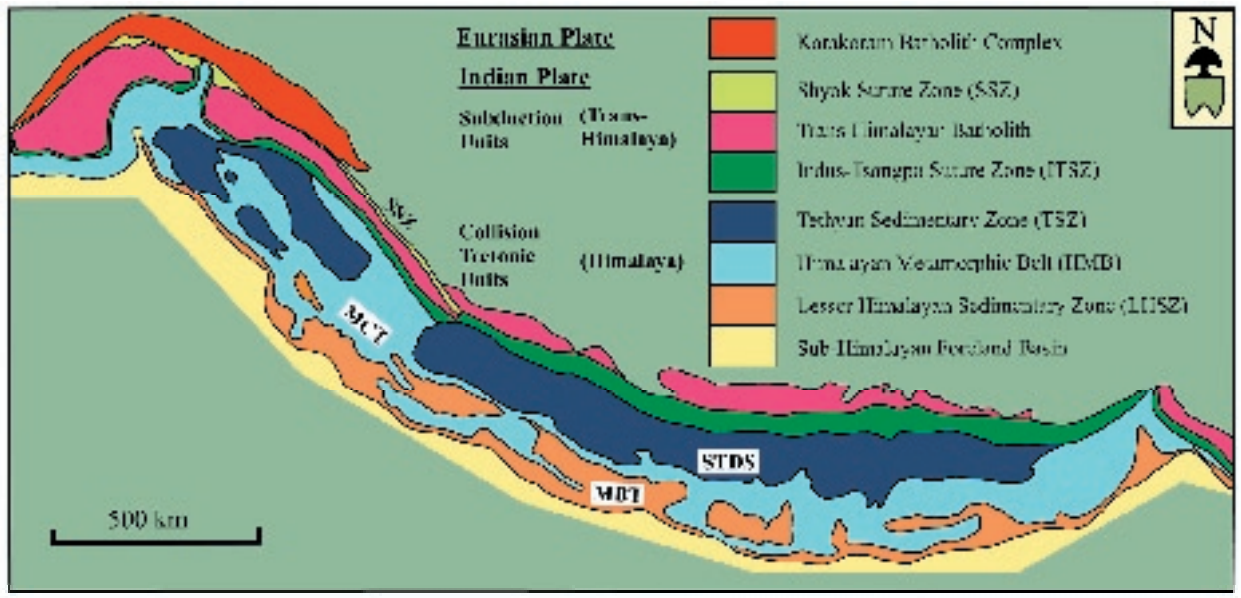

Figure 1. Simplified regional geological framework of the Himalaya in plate tectonic framework. Abbreviations: SSZ-Shyok Suture Zone. ITSZ-Indus Tsangpo Suture Zone. THSZ/STDZ-Trans Himadri Shear Zone/South Tibetan Detachment Zone. MCT-Main Central Thrust. MBT-Main Boundary Thrust. Complied from published data.

has been postulated (Debon et al. 1986; Le Fort, 1986; Searle and Rex, 1989; Hodges et al., 1992).

This contribution is an attempt to constrain the source characterization and possible emplacement mechanism of the collision-related Gangotri Leucogranite along Bhagirathi Valley, NW-Himalaya, India.

Geological Framework

The Gangotri Granite is the western end of the Badrinath Granite as one of the largest bodies of the High Himalayan Leucogranite (HHL) belt in the Garhwal Himalaya. It is exposed along the upper reaches of the Bhagirathi River in the Gangotri glacier region, including the peaks of Thalay Sagar (6904 m), Bhagirathi (6856 m), Meru Parbat (6672 m), Shivling (6543 m) and Bhigupanth (6044 m). The granite was first described by Heim and Gansser (1939) from the Higher Himalaya along upper Alaknanda Valley near Badrinath. Later, Auden (1949) described fine grained tourmaline +muscovite+biotite+garnet granite from the upper Bhagirathi Valley and termed it the Gangotri Granite.

In the Gangotri region, two types of granitoids have been described from the upper reaches of the Bhagirathi River (Fig. 3; Pant, 1986; Pant and Dave, 1994). The Gangotri Granite is made up of several lenses or small leucogranite plutons, which are 1.5-2 km thick and 4-5 km long (Scaillet et al., 1990; Searle et al., 1993, 1999) in contrast to the single large Manaslu pluton. These lenses intrude either the metamorphosed base of the Tethyan Sedimentary Zone (Martoli Formation), the Harsil Formation (Pant, 1989), or occur in a large body of two-mica megacrystic granite, which has been named the Bhaironghati Granite (Pant, 1989). The latter also intrudes the quartzo-feldspathic gneiss and schist of the HHC below and the Martoli Formation above. The emplacement of a number of en-echelon lenses of granite bodies around Gangotri and further southeast appears to have taken place along an extensional shear zone near the top of the HHC (Searle et al., 1993).

Stern et al. (1989) conducted Rb-Sr measurements on the whole rock and mineral separates (two-feldspar, muscovite and tourmaline) from the Gangotri Granite, and observed significant scattering on the isochron diagram. The Gangotri Granite, also known as the Badrinath body, is composed of several bodies. Deep incision by the Bhagirathi River provides different exposures of these bodies at Shivling, Bhagirathi, Meru and Thalay Sagar peaks. The whole rock analyses of leucogranite have yielded a 5-point Rb-Sr isochron of 21.1±0.9 Ma (Stern et al., 1989). However, Th-Pb monazite gave an age of 22.4±0.5 Ma for the Gangotri and 21.9±0.5 Ma age for the Shivling leucogranites (Harrison et al., 1997b). Searle et al. (1999) obtained a U-Pb monazite age of 23.0±0.2 Ma for the Shivling body. All these ages have been interpreted as the recrystallization age for the Gangotri-Badrinath group of leucogranites in the Garhwal Himalaya. Cooling ages for the Gangotri Granite were found to be 17.9±0.1 Ma using $^{40}Ar/^{39}Ar$ method for muscovite and between 2.41±0.52 Ma and 1.48±0.60 Ma by fission track dating of zircon and apatite, respectively for a temperature range between 350±50ºC and 130±10ºC (Sorkhabi et al., 1996, 1999).

Field Settings

The Gangotri Granite intrudes both the Bhaironghati Granite and the Martoli Formation of the Tethyan Sedimentary Zone. Field observations indicate that a network of aplite-pegmatite dykes and the Gangotri Granite cross-cut the foliation of the biotite granite gneiss and metasedimentary host rocks. The contacts between the two granites are always sharp. However, leucogranite lenses can be traced for a few kilometres along cliffs of biotite granite/gneiss. Overall, these observations indicate

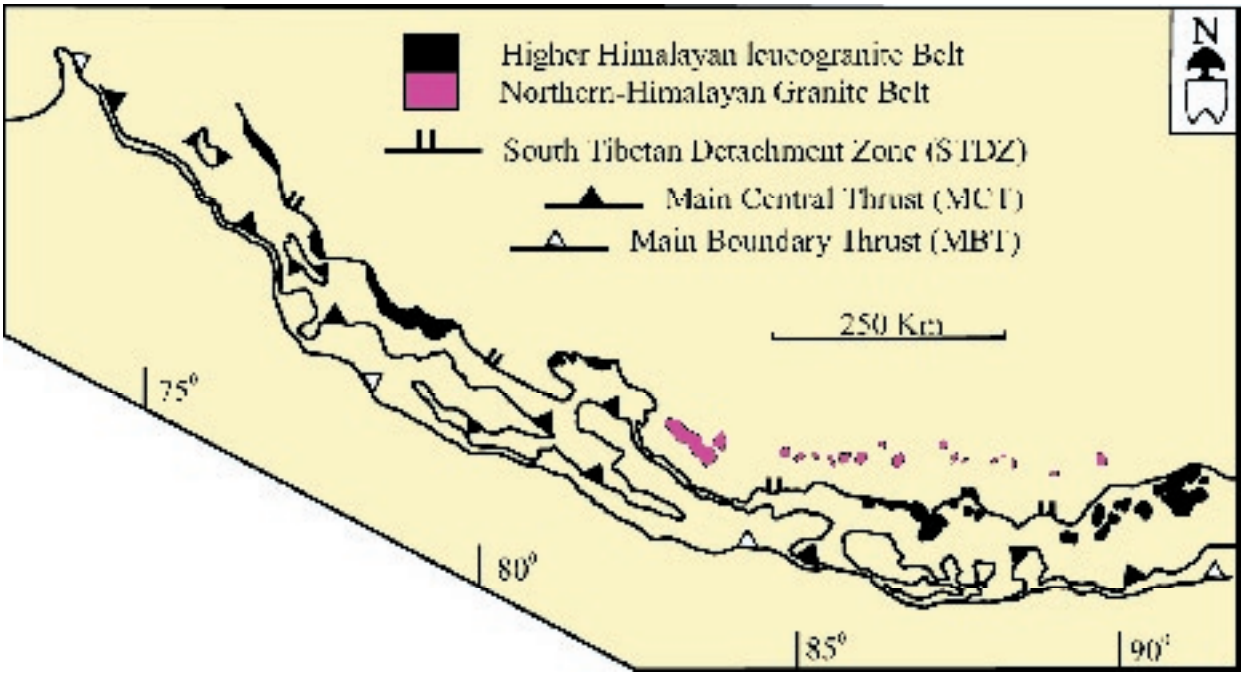

Figure 2. North Himalayan and Higher Himalayan granitoid belts. 1-Lesser Himalayan Proterozoic Belt. 2-Himalayan metamorphic Belt (HMB).

a late-to post-metamorphic emplacement of the Gangotri Granite.

Along the main road section from Jangla to Gangotri and beyond, two distinct granites occur, i.e. the biotite granite/gneiss and tourmaline-bearing leucogranite. At the Jangla Bridge, biotite granite is deformed into a medium to coarse-grained granite gneiss at the lower structural levels, close to the contact with the Harsil metamorphics. It extends along the northern slopes of the Bhagirathi Valley between Sian Gad, Harsil and Mukba. This granite is strongly foliated to granite gneiss at the contact with the metamorphics, but the main body remains undeformed and is medium to coarse grained and equigranular with occasional xenoliths. Numerous veins of tourmaline-muscovite leucogranite and garnet-beryl-tourmaline pegmatite intrude the biotite granite and the metamorphics. The Bhairoghati Granite contains mainly quartz+ orthoclase+ perthite+ microcline+ plagioclase+ biotite±muscovite ±zircon±apatite± epidote. Feldspar margins are sheared recrystallized and foliated and, at times, developed myrmekite.

The structure of the Gangotri Granite is usually characterized by a very weak foliation, defined by mica and tourmaline. Near the contacts, the foliation grades into layering which includes a few cm thick bands of tourmaline. Two kinds of xenoliths are present within the leucogranite. The most abundant ones, always located near the contacts, are angular pieces of the host rock, which are often up to several meters in length. This results into the subparallel upper contact with the overlying black slates of Martolis, which are metamorphosed into the staurolite grade around Bhagirathi and Thalay Sagar peaks (Stern et al., 1989).

The temple at Gangotri is built up on the tourmaline-bearing leucogranite. The body is fine-grained, massive, northerly-dipping sheet-like lens, having preferred oriented tourmaline crystals, which generally develop perpendicular to the wall of the granite body. It is dissected by set of steep to vertical joints through which the Bhagirathi River and the Jadh Ganga cascade down and cut extremely narrow gorges.

The Gangotri Granite is very homogenous, and texturally equigranular and hypidiomorphic. The body contains quartz+ feldspar+ muscovite+ tourmaline± opaque± apatite± biotite± monazite± zircon± garnet. Both tourmaline and muscovite are of magmatic origin. The accessory minerals are randomly oriented in an overall quartz-orthoclase mosaic. The inferred crystallization sequence is characterized by the early appearance of plagioclase, quartz and biotite, and late crystallization of the k-feldspar. It appears to be in the near-minimum melt composition, as their plot cluster around the invariant point in kf-Q-Plag-H_2O diagram (Johannes and Holtz, 1990).

Geochemistry

Twenty nine granitoid samples from the Bhairoghati Granite and Gangotri Granite have been analysed for their major and trace elements using standard WD-XRF technique. Seven samples among them, collected along Bhagirathi and Jadh Ganga valley (Fig. 4) were also critically chosen and analysed for their REE abundance by ICP-AES technique (Rathi et.al. 1996). The details of the analytical procedures, sample preparation and instrumental conditions are mentioned in Saini et al. (2002) for XRF analysis and Rathi et al. (1996) for REE analysis.

The Gangotri Leucogranite (LG) shows a rather restricted range of major and trace elemental abundance as compared to the Bhairoghati Granite (BG), also referred to as biotite granite, (Table 1 & 2). Analyses of major elements of these granitoids indicate that these are peraluminous in character, having Al_2O_3/Na_2O+K_2O+CaO ratio >1.1(Zen 1986, Chappel and White, 1992). Major elemental abundances show strong correlations with SiO_2 notably having a negative trend for CaO representing in assimilation and early crystallization of calcic plagioclase

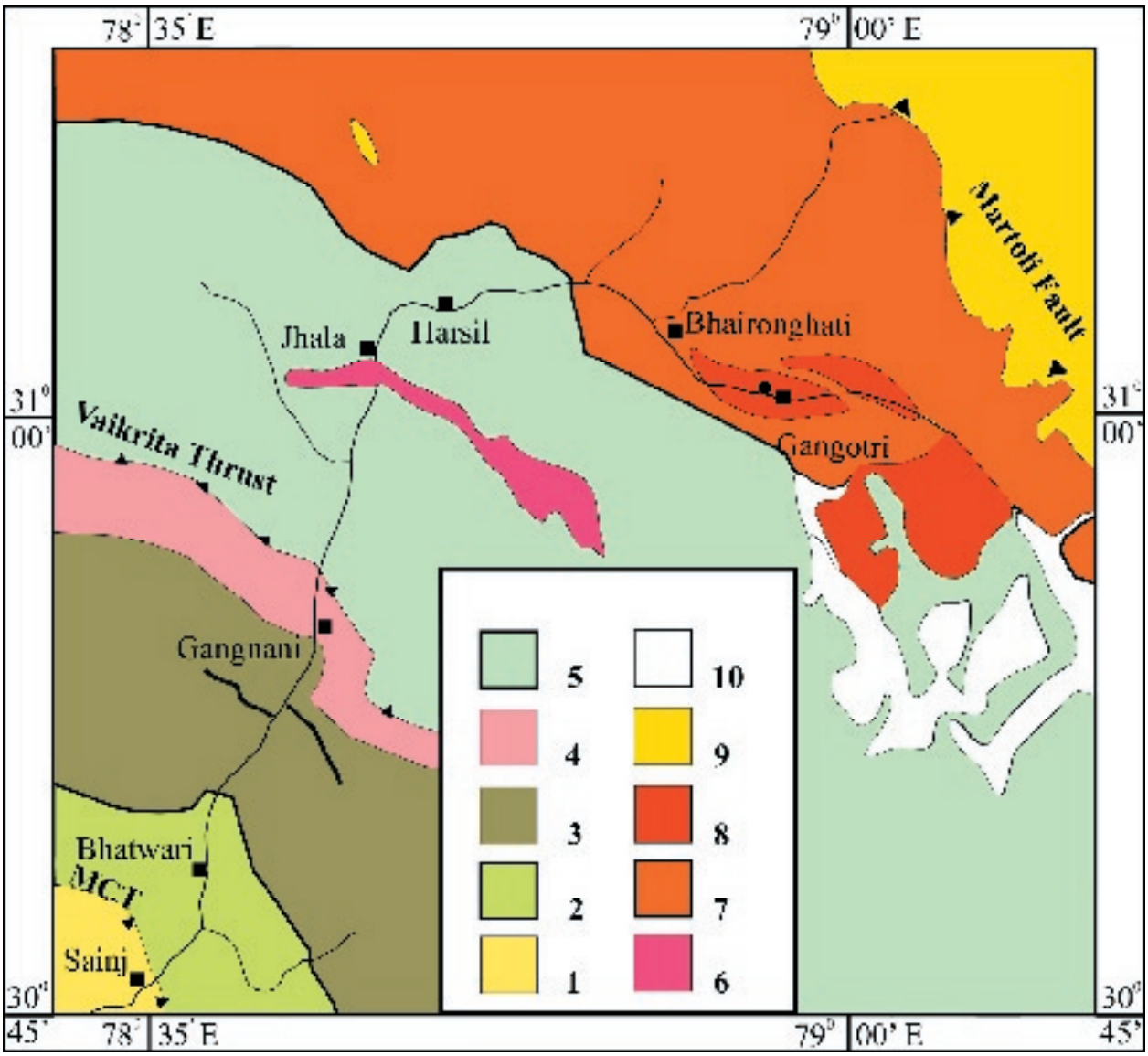

Figure 3. Geological map of the Higher Himalayan Crystalline (HHC) Belt along the Bhagirathi Valley, Garhwal. Legend: 1: Lesser Himalayan (LH) Proterozoic sequence; Higher Himalayan Crystallines (HHC) 2: Bhatwari Group-porphyroclastic granite gneiss, garnetiferous mica schist, amphibolite, 3: mylonitized augen gneiss, mica schist, amphibolite, 4: phyllonite, schist, 5: sillimanite/kyanite/staurolite/garneti-ferous schist/gneiss/ migmatite, 6: angen gneiss, 7: Bhaironghati granite, 8: Gangotri leucogranite. 9: Tethyan Sedimentary Zone (Martoli Group). 10: Glaciers, debric etc. Abbreviations: MCT - Main Central Thrust, VT - Vaikrita Thrust, MF - Martoli Fault.

in these granites (Fig. 5 a). The biotite granite has higher FeO+ MgO, TiO_2 and Ni content than the leucogranite; the overall decreasing trend of FeO (t) and MgO as SiO_2 increases suggests high fractionation of mafic minerals like biotite, magnetite etc. (Figs. 5 b, c). Low abundance and less spread of these elements in case of leucogranite indicate lower abundance of mafic minerals and their insignificant role in fractional crystallisation. There is no systematic pattern of P_2O_5 with SiO_2, which reveals formation of apatite at all stages of crystallization in biotite granite, however, the range of P_2O_5 in leucogranite is very narrow (Fig. 5 d). There is an apparent negative correlation between TiO_2 and SiO_2 in biotite granite indicating role of Fe-Ti oxide and biotite in the fractionation process. (Fig.5 e). However, there is no distinct trend between Al_2O_3 and SiO_2, except a feeble negative correlation in leucogranite indicating formation of feldspar (Fig. 5 f). The LG are strongly enriched in SiO_2, alkalies and alumina and depleted in CaO. There is a positive correlation of SiO_2 and Na_2O mainly in case of leucogranite (Fig. 5 g). No possible correlation exists between MnO and SiO_2 in both the granitoids (Fig. 5 h). Several geochemical trends were earlier noted by Scaillet et al. (1990) from main body of the Gangotri Granite where an increase in Na_2O, Rb, Sr, U, B and F, and a decrease in K_2O, Fe_2O_3, TiO_2, Sr, Ba, Zr, REE and Th were noticed with decrease in CaO content. These variations can be best explained by the fractionation process of appropriate phases. Experimental solubility models for zircon and monazite in felsic melt support a magmatic origin for these two accessory phases as well (Scaillet et al., 1990). A tight correlation between Zr-TiO_2 strongly supports zircon hosted biotite fractionation in case of biotite granite (Clark et al. 1993).

Steep depletion of Sr as a function of SiO_2 in biotite granite indicate extensive fractionation of plagioclase (Fig.6 a), whereas, that of Rb, which initially increases and then depletes (Fig.6 b), suggesting appearance of K-feldspar at later stage. However, the overall pattern of Rb

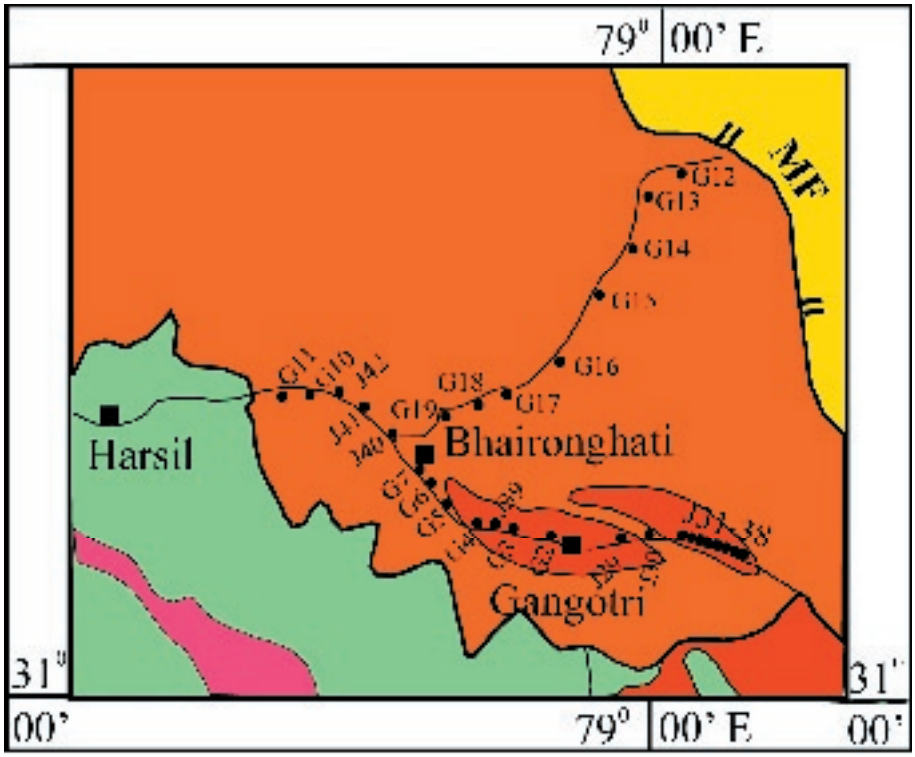

Figure 4. Enlarged portion of Figure 3 for showing sample location of the geochemical analysis.

vs. Sr indicates that the crystal fractionation is a viable mechanism for trace elemental variation in biotite granite (Fig. 6 c). Low Zr in leucogranite as compared to biotite granite indicates that there is little formation or saturation of zircon did not reach in leucogranite (Fig. 6 d). It also follows that the degree of partial melting of felsic source and temperature was very low resulting in abundance of restitic zircon in the source. Spidergram plot of biotite granite and leucogranite show almost similar trend, except the difference in abundances (Figs. 7 a & b). In biotite granite, Zr shows a positive trend indicating presence of zircon, whereas it has a negative anomaly in leucogranite. Also, P shows a large scattering in the former, whereas it has a restricted range and positive anomaly in leucogranite indicating precipitation of apatite within the accessories phases in biotite granite but same is not apparent in case of leucogranite. The observed high negative anomaly of Th and variation in U probably indicate involvement of monazite as residual phase in the generation of leucogranite.

In the present study, all the REE analyses (Table 3) were normalized to C1 Chondrite values and plotted in Figure 8. The Gangotri Granite shows lower LREE and HREE abundances as compared to the biotite granite. However, these show almost similar trends and are enriched in LREE and depleted in HREE. The BG possess steeper slope in LREE and gentler slope in HREE having slight concave trend and reveal that these bodies are moderately fractionated in HREE with respect to LREE. However, in case of LG, the HREE is more prominantly depleted. BG samples are also characterized by a strong negative Eu anomaly - an indication of fractionation of plagioclase. The Eu anomaly in case of LG is rather weak suggesting limited feldspar fractionation. Low Yb concentration and moderately fractionated REE pattern of LG suggest that these granites are derived from a crustal source, which is further supported by Rb vs. Y+Nb plot of Pearce et al. (1984), in which these bodies fall well within syncollisional domain (Fig. 9).

Geochronology

Whole-rock Rb/Sr isotopic ratios for biotite granite/gneiss and leucogranite have been attempted (Singh, 1986; Stern et al., 1989; Scaillet et al., 1990). The data given by these workers were recalculated and plotted on $^{87}Rb/^{86}Sr$ vs. $^{87}Sr/^{86}Sr$ plot by us. Two-error regression of data was made using computer programme, based on Wendt's Model II (1969).

$^{87}Rb/^{86}Sr$ ratios of whole rock samples from the biotite granite/gneiss (Singh, 1986) have been plotted against $^{87}Sr/^{86}Sr$ values on Sr evolution diagram (Fig. 10 a). The two-error regression analysis of data yields an isochron age of 528.47±23.08 Ma with an initial $^{87}Sr/^{86}Sr$ ratio 0.710212±0.00033 and mean square of weighted deviation 0.78 and correspond to the Cambro-Ordovician (500±50 Ma) Pan-African magmatic event in the Himalaya. It may be of interest to note that Kwatra et al. (1999) have obtained 5-point whole rock Rb-Sr isochron age for the adjoining Raksham and Akpa granitoids of the Baspa-Sutlej Valleys as 453±8.84 and 477.29±29 Ma, respectively.

Stern et al. (1989) have published repeat Rb-Sr isotopic measurements on six whole-rock samples of the Gangotri Granite with an isochron age of 63.66±9.54 Ma with an initial $^{87}Sr/^{86}Sr$ ratio of 0.746645±0.00014 and MSWD value of 0.06 (Fig. 10 b). Later, Scaillet et al. (1990) have obtained eight whole-rock Rb-Sr isotopic measurements from the Bhigupanth, Bhagirathi, Gangotri and Shivling

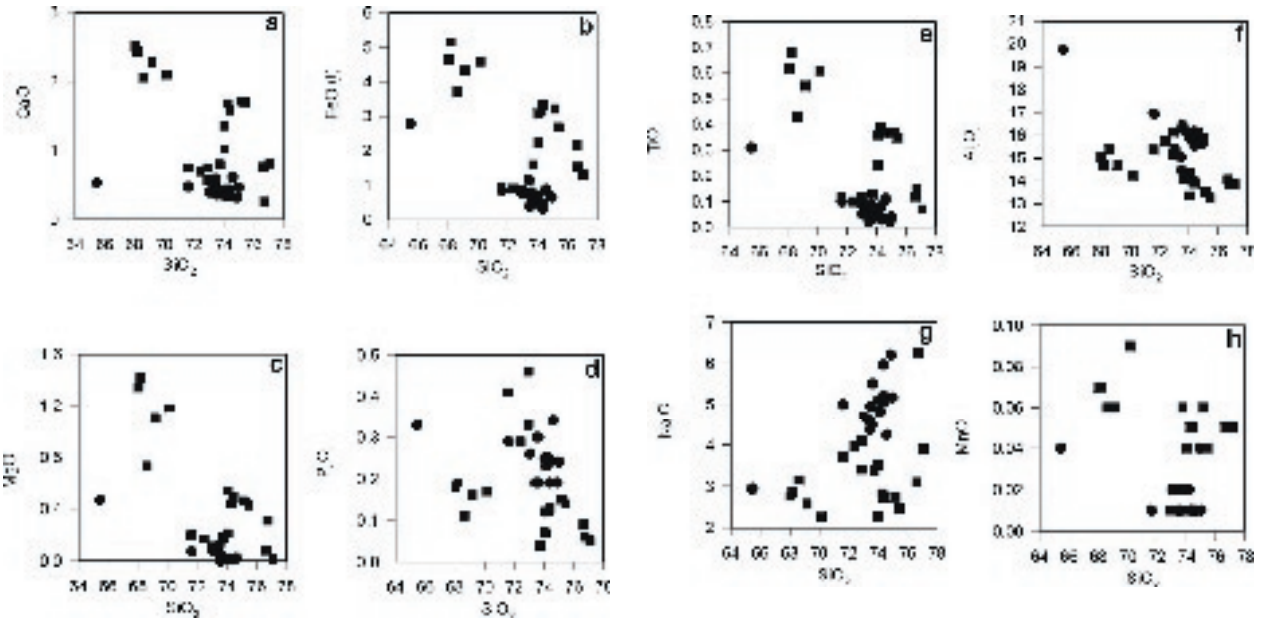

Figure 5. Harker diagrams showing correlation between SiO2 and (a) CaO, (b) FeO (t), (c) MgO, (d) P2O5, (e) TiO2, (f) Al2O3, (g) Na2O, and MnO.

plutons. The data obtained by them have a significant scattering on isochron diagram, but the regression line define an age of 51.25±9.09 Ma with MSWD value 1.92, and an initial $^{87}Sr/^{86}Sr$ ratio of 0.764525±0.00013 (Fig. 10 c).

We have attempted to combine the data published by Stern et al. (1989) and Scaillet et al. (1990). The data show a considerable scattering on the isochron diagram and the two s-error regression line yields an age of 57.05±6.72 Ma with an initial $^{87}Sr/^{86}Sr$ ratio 0.756109±0.0001 and the MSWD value 4.03, which is on the much higher side (Fig. 10 d). This shows a high level of isotopic variation, which could be either due to inhomogenity during initial stages of pluton formation or that the system have become open after its emplacement. However, it is evident that the intrusive age of the Gangotri Granite is not constrained by the above data. Recently, Harrison et al. (1997) obtained the Th-Pb monazite ages for the Gangotri Granite from the proper Gangotri as 22.4±0.5 Ma and Shivling as 21.9±0.5 Ma. This matches with the five-point Rb-Sr mineral isochron of 21.1±0.9 Ma by combining the whole rock with two feldspars, muscovite and tourmaline (Stern et al., 1989). Further, Searle et al. (1999) obtained U-Pb age of 23.0±0.2 Ma for Shivling leucogranite. The age of 22-23 Ma for the Gangotri Granite appears to be more appropriate and almost corresponds to the emplacement age of numerous Early Miocene Himalayan leucogranites.

Systemic cooling and exhumation rates of the Gangotri Granite have been calculated recently after initial determination of muscovite K-Ar ages of 18.4±0.7 Ma and 18.9±1.3 Ma by Seitz et al. (1976) from a leucogranite sample from the Badrinath, and by Stern et al. (1989) from the Bhagirathi leucogranite as well as Rb-Sr mineral age of 21 Ma. Subsequent $^{40}Ar/^{39}Ar$ dates on muscovite separates from leucogranite at Gangotri yield a plateau age of 17.9±0.1 Ma; and biotites from the biotite granite about 800 m above the former gives a similar age of 18.0±0.1 Ma (Sorkhabi et al., 1999). A total of 15 apatite fission track ages from a cliff section above the Gangotri temple on the left bank of the Bhagirathi River between 2670 and 4370 m give an age range from 1.48±0.6 Ma to 2.41±0.52 Ma with a weighted mean of 2.0±0.52 Ma, ~2 mm/yr exhumation rate and 63-70ºC/Ma cooling rate. This fast cooling and exhumation rates contrast with 10-13ºC/Ma cooling and 0.38 mm/yr exhumation rates from ~18 Ma to 2 Ma (Jain et al., 2000). Since the crystallization of the Gangotri Granite at 22 Ma, cooling and exhumation rates had been 80ºC/Ma and ~ 3 mm/yr, respectively (Fig. 11).

Petrogenesis of HHL

The peraluminous Himalayan S-type Cenozoic leucogranites within the HHC of the Zanskar-Garhwal-Nepal-Bhutan have originated crustally either partly or wholly from the basement, which is composed of metamorphics, migmatites and Early Paleozoic granites and having distinct variations along the regional trend of the Himalayan orogen (cf. Le Fort et al., 1987; Daniel et al., 1987; Pognante et al., 1987; France-Lanard et al., 1988). These granitoids are generally more homogeneous large plutons intruding the higher stratigraphic and structural levels in the east. Different P-T-t paths have been observed in association with the leucogranite (Pognante, 1993), who has argued an important role of liberated fluids during metamorphism. He has also argued that decreasing pressure conditions from west to east across the Indian Plate is one of the main factors, which has controlled the increased abundance of leucogranites in Nepal. It has also been observed that there is a relatively high pressure anatexis in NW Himalaya, hence smaller leucogranite amounts are generated in contrast to Nepal. As such, low degree of partial melting has partly inhibited the accumulation and ascent of the leucogranite melt, which therefore, remained in place to form in situ migmatites and leucogranite.

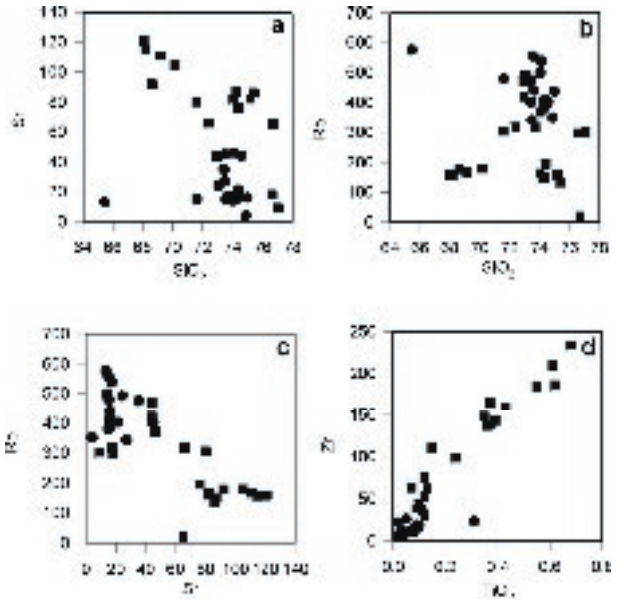

Figure 6. Harker diagrams showing correlations between (a) SiO2 and Sr, (b) SiO2 and Rb, (c) Sr and Rb, and (d) TiO2 and

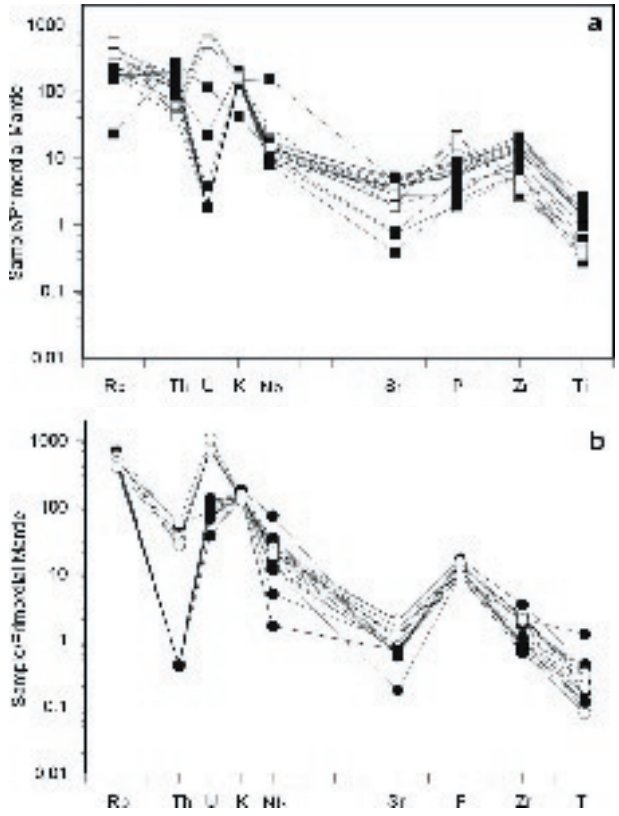

Figure 7. (a) Spidergram of trace elements from the Bhaironghati granites (solid squares) and the Gangotri granite (empty squares). All samples normalized to primordial mantle. (b) Same as above from Scaillet et al. (1990). Bhairoghati granite (solid circles), Gangotri Granite (empty circles).

Different models have been put forward for possible origin of the High Himalayan leucogranites. The tectonic model for the generation and emplacement of these granitoids has been suggested by Le Fort (1975, 1981, 1986) and Le Fort et al. (1987). This model combines thrusting on a continental scale along the Main Central Thrust (MCT) with development of inverted metamorphism and liberation of large quantities of fluids, thus causing anatectic melting of the crust. Thrusting along the MCT brings hot portions of the deep continental crust, the Tibetan Slab, over the little metamorphosed Midland Formation (Lesser Himalayan rocks) in Nepal. This continuous process heats the latter from top to bottom and induces synkinematic inverted metamorphism. In turn, dehydration and decarbonation metamorphic reactions release large amount of fluids that rise above the MCT. In the portion of the Tibetan Slab that is hot, these fluids induce anatexis and produce melts close to the minimum melt compositions. This melt is then emplaced at higher levels at the top of the Tibetan Slab.

Searle and Fryer (1986) proposed that frictional heating was not compatible due to the high water and volatile contents and requires dry melt. They suggested that crustal anatexis has caused migmatization and subsequent intracontinental subduction liberated large quantities of fluids, which induced the melting. This melt crystallized tourmaline and muscovite with garnet, feldspar, and quartz. These boron-rich fluids induced the melting by lowering the solidus, and therefore, making the magma less viscous.

The mechanism of intrusion for the Higher Himalayan leucogranites are influenced by such factors like composition, volume, viscosity, water content of the magma and the state of stress in the Higher Himalaya. It has been argued that the emplacement mechanism of the leucogranites is mainly related to their level in crust (Searle et al., 1988; Searle and Rex, 1989; Searle, 1991). According to Searle (1991), deeper structural levels are associated with partial melting producing migmatites and layered granite sheets as well as remobilization of granite; whereas mid-crustal levels are characterized by sheet-like intrusions along fluid-rich ductile shear zones as a result of melt-enhanced deformation (Hollister and Crawford, 1986). High structural levels are characterized by migrated plutons that originate from deep levels of the crust but have intruded upwards and cross cutting the regional metamorphic isograds.

The simplest model, as could be proposed for the leucogranite formation, has been mainly or completely derived from anatexis of continental crust during the Himalayan collision tectonics, which has resulted in the crustal thickening and the isostatic readjustments. It has resulted into the depression of the base of the continental block, which is forced into a higher temperature environment, causing melting of the lower crustal rocks.

Discussions

The Higher Himalayan Leucogranite (HHL) Belt is a result of the collisional related magmatism having strong peraluminous character with presence of muscovite and tourmaline along with uniform minimum-melt compositions (Kai, 1981; Le Fort et al., 1987; Inger and Harris, 1993; Harris et al., 1993; Gulliot and Le Fort, 1995, Searle et al., 1997). The two-mica leucogranites are found in practically all-orogenic belt as a result of syntectonic anatexis process of the crust. The regional Barrovian Himalayan metamorphism gave an anti-clockwise P-T

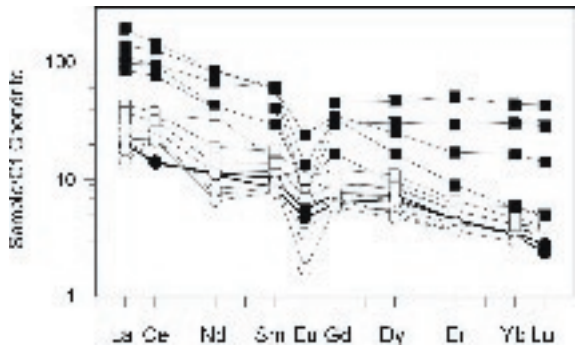

Figure 8. REE pattern of the Bhaironghati (solid squares) and Gangotri granites (empty squares). All samples normalized to C1 Chrondrite. Also shown is the data from both the bodies (circles), obtained by Scaillet et al. (1990).

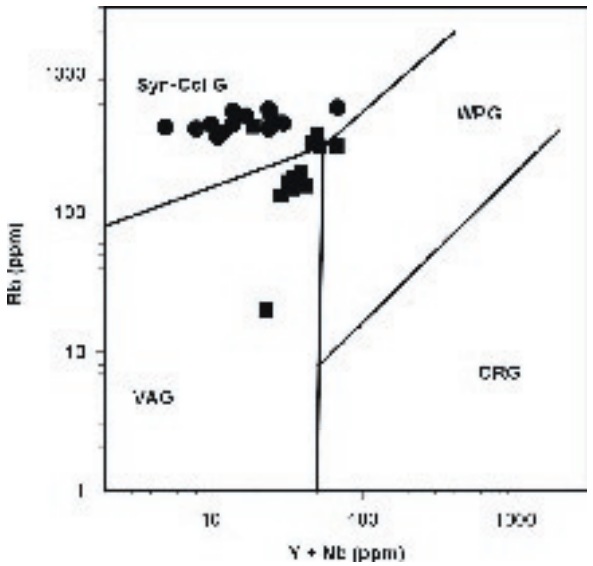

Figure 9. Rb vs. Y+Nb plot of Pearce et al. (1984) showing Bhaironghati granite (square) and syn-collisional Gangotri Granite (circles).

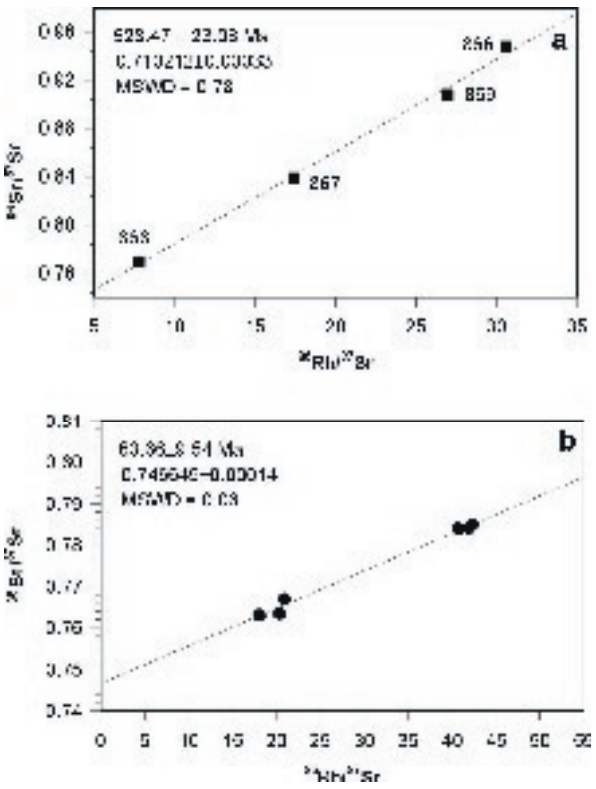

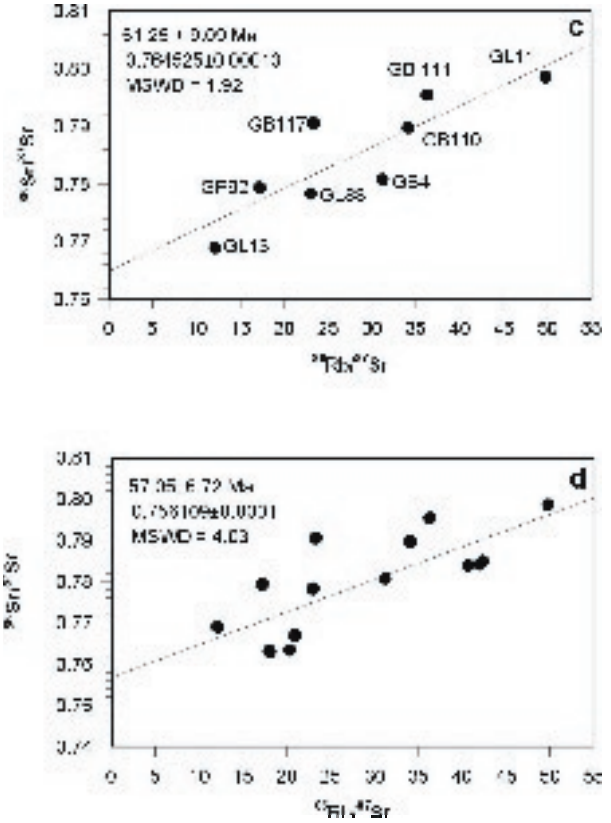

Figure 10 (above & right). Rb/Sr whole-rock isochron diagram for the (a) Bhairoghati granite (Singh, 1986), (b) Gangotri Granite (Stern et al., 1989), (c) Gangotri Granite (Scaillet et al., 1990), and (d) Combined Rb/Sr whole-rock isochron diagram for the Gangotri Granite.

path (for summary see Gulliot et al., 1999 and Jain et al., in press) deduced from medium and high-grade zones due to the crustal thickening. Thickening of the crust induced a tectonic denudation by collapse of the upper terrain inducing a short-lived tectonic burial followed by exhumation. The exhumation during Miocene time caused the decompression melting causing anatexis.

The metamorphism led to the formation of anatectic migmatites in the upper level of Higher Himalayan Crystallines (HHC) and intrusion of leucogranite magma as both insitu incipient melting and emplacement of large-scale sheets and sills of crustally derived intrusive. The observed isotopic signatures (Sr, Nd and Pb) on the HHL belt (Vidal, 1978; Denial et al., 1987; Gareipy et al., 1985) along with the experimental data (Scaillet et al., 1995; Patinio Douce and Harris, 1998) indicate the source could be metasedimentary. The geochronological data on the Higher Himalayan Leucogranite (HHL) belt suggest that they have been emplaced between older 24 Ma and younger 17 Ma episode (Noble and Serale, 1995; Harrisson et al., 1997, 1999; Searle et al, 1997, 1999). Though the ages vary, but the major phase of leucogranite occurred by dehydration melting between 24-22 Ma.

The formation of HHL Belt is a matter of debate among the workers. Mainly three interpretations have been put forward; the first interpretation is that the HHL has

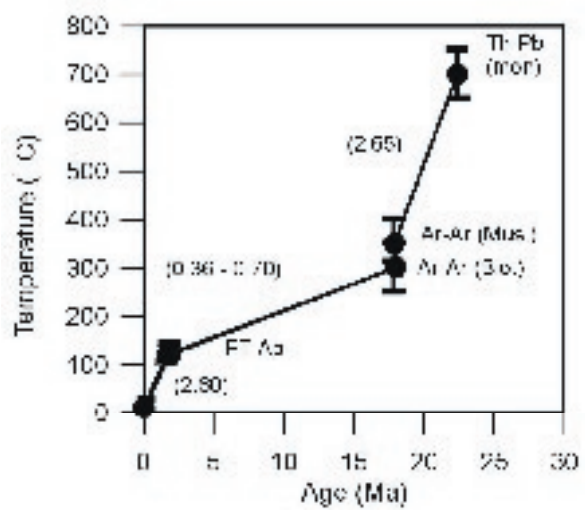

Figure 11. Exhumation rates of the Gangotri Granite using Th-Pb monazite, Ar-Ar muscovite-biotite and FT apatite systematics (Jain et al., 2000).

along the STDS but may not have been synchronous with motion on the MCT. Harris et al. (1993) proposed that the HHL were produced by high-temperature muscovite dehydration melting and became mobile only after tectonic decompression (via the STDS) marked increased melt fraction. Here the decompression melting along the footwall of STDS has been cited as the main process responsible for the formation of the leucogranite. Furthermore, recent experimental evidence indicates that water-saturated melting of the Himalayan source rock produced melt of Trondhjemite rather than leucogranite composition (Patino Douce and Harris, 1998). The third interpretation indicate that the HHL belt could be linked to shear heating on a continous active devolvement and cuts through Indian Supra-crustal rocks that were transformed into basement during initial stages of the Indo-Asia collision (Harrisson et al., 1997, 1999). Decompression above cannot trigger the melting rather this mechanism could work in concert with fraction heating along a thrust surface and the anatexis resulted from vapour-absent muscovite dehydration melting of HHC. They represented the integrated melting properties of the source region by averaging experimental determined melting relationship for various metasedimentary composition (Gardien et al., 1995), which is closely related to muscovite and biotite dehydration melting (Le Preton and Thompson, 1988).

Summary & Conclusions

The depleted strontium and CaO, high silica and Na_2O content together with narrow range of major elemental and trace elemental abundance in LG implies that there is not much variation of degree of partial melting. Tight felsic compositional range may represent minimum melt composition of a felsic source with abundant feldspar, thus precludes the possibility of the melt generation from pelitic meta-sedimentary source. The high-grade meta-sedimentary rocks and associated migmatites in the proximity of the LG also show contrasting geochemistry. The observed linearity in binary variation diagram and sub-parallel nature of the REE and spider-diagram pattern of the LG with the BG suggests that BG to be most potential candidate as the source for generation LG melt. This is also consistent with the field disposition of the two granitoids bodies in this area.

The more albitic plagioclase in LG suggest incongruent low fraction partial melting of BG, in which the Na-rich component of plagioclase partitioned into melt leaving behind Ca-rich more anorthitic plagioclase in the residue. This has also resulted in depleted Sr content in LG, which preferentially retained by restitic plagioclase. Similarly, the incongruent melting of K.f. would produce K-rich melt and therefore the melt would also be enriched in Rb as observed in LG. In case of higher degree of partial melting, these signatures would get diluted and therefore, we suggest that the LG was produced by lower degree of partial melting probably at shallower depth and low temperature. The pH_2O requirement for low temperature melting was probably met internally by dehydration reaction of abundant hydrous phases like biotite and muscovites and intergranular water dissolved at grain boundaries (Pichavant et al. 1988, Pichavant and Montel, 1988). The observed low Zr further substantiates this and hence more depleted HREE that results from the non-involvement of refractory minerals like zircon, probably also monazite, in the melting process.

The problem of separation of low fraction felsic melts from the source due to high viscosity has been discussed in detail by Wickman, (1987). It is suggested that a interconnected low fraction felsic melt can only be separated from the residual source by compaction (Jurewicz and Watson, 1984, 1985). Since the LG are related to syn-collisional events, the compactional or shearing stress enabled the felsic melt fraction to separate from the source region.

Acknowledgements

The present work was carried out under Department of Science and Technology sponsored projects to SS and AKJ over the years. It took us a long time to finalize it through the opportunity given by Virtual Explorer in the form of edited volume on Granitoids of Himalayan Collisional Belt. We thank Director, Wadia Institute of Himalayan Geology for extending facilities of XRF and ICP for geochemical analysis. We also thank Drs. K.R. Gupta, RM. Manickavasagam, M.S. Rathi, R.S. Sharma, Rasoul Sorkhabi, Nand Lal for constant support and encouragement throughout the work.

References

Auden, J.B. (1935) Traverses in the Himalaya. Rec. Geol. Surv. India, v. 69, pp. 123-167.

Auden, J.B. (1949) General report of G.S.I. for 1939. Rec. Geol. Surv. India, v. 78, pp. 74-78.

Chappel, B.W. and White, A. J. R. (1992) I- and S- type granites in Lachland Fold belt. Trans. Royal. Soc. Edinberg (ES) v. 83, pp. 1-26.

Clark, DB., Macdonald, MA., Reynolds, PH., and Longstaffe, FJ., (1993). Leucogranites in the Lachlan fold belt. Trans. R.

Soc. Edinburg (ES), v. 83, pp. 1-26.

Debon, F., Le Fort, P., Sheppard, S.M.F. and Sonet, J. (1986) The four plutonic belts of the Transhimalaya-Himalaya: A chemical, mineralogical, isotopic and chronological synthesis along a Tibet-Nepal section. J. Petrol., v. 27, pp. 219-250.

Deniel, C., Vidal, P., Fernandez, A., Le Fort, P. and Peucat, J.J. (1987) Isotopic study of the Manaslu granite (Himalaya, Nepal): Inferences on the age and source of Himalayan leucogranites. Contrib. Miner. Petrol., v. 96, pp. 78-92.

England, P., Le Fort, P., Molnar, P. and Pecher, A. (1992) Heat source for Tertiary metamorphism and anatexis in the Annapurna-Manaslu region (central Nepal). J. Geophys. Res., v. 97, pp. 2107-2128.

France-Lanord , C. and Le Fort, P. (1988) Crustal Melting granite and genesis during the Himalayan collision orogenesis. Trans. R. Soc. Edinburgh (Earth Sci.), v. 79, pp. 183-195.

France-Lanord, C., Sheppard, S.M.F. and Le Fort, P. (1988) Hydrogen and oxygen isotope variations in the High Himalaya peraluminous Manaslu leucogranite: evidence for heterogeneous sedimentary source. Geochim. Cosmochim. Acta, v. 52, pp. 513-526.

Gardien, V., Thompson, A.B., Grujic, D. and Ulmer, P. (1995) Experimental melting of biotite + plagioclase + quartz ± muscovite assemblages and implications for crustal melting. Jour. Geophys. Res., v. 100, pp. 15581-15591.

Gareipy, C., Allegre, C.J. and Xu, R.H. (1985) The Pb-isotope geochemistry of granitoids from the Himalaya-Tibet collision zone: implications for crustal evolution. Earth Planet. Sci. Lett., v. 74, pp. 220-234.

Griesbach, C.L., 1893. Notes on the Central Himalaya. Rec. Geol. Surv. India, v. 26, pp. 19-25.

Gulliot, S. and Le Fort, P. (1995) Geochemical constraints on the bimodal origin of High Himalayan leucogranites. Lithos, v. 35, pp. 231-234.

Gulliot, S., Cosca, M., Allemand, P. and Le Fort, P. (1999) Contrasting metamorphic and geochronologic evolution along the Himalayan belt. In: Macfarlane, A., Sorkhabi, R.B. and Quade, J. (Eds.) Himalaya and Tibet: Mountain roots to mountain tops. Geol. Soc. Amer. Spec. Paper 328, pp. 117-128.

Harris, N. and Massey, J. (1994) Decompression and anatexis of Himalayan metapelites. Tectonics, v. 13, pp. 1537-1546.

Harris, N., Inger, S. and Massey, J. (1993) The role of fluids in the formation of High Himalayan leucogranites. In: Treloar, P.J. and Searle, M.P. (Eds.) Himalayan Tectonics. Geol. Soc. London Spec. Publ. No. 74, pp. 391-400.

Harrison, T. M., Lovera, O.M. and Groove, M. (1997) New insights into the origin of two contrasting Himalayan granite belts. Geology, v. 25, pp. 899-902.

Harrison, T.M., Grove, M., Lovera, O.M., Catlos, E.J. and D'Andrea, J. (1999) The origin of Himalayan anatexis and inverted metamorphism: Models and constraints. J. Asian Earth Sci., v. 17, pp. 755-772.

Heim, A. and Gansser, A (1939) Central Himalaya- Geological observations of Swiss Expedition 1936. Mem. Soc. Helve. Sci. Nat., v. 73, 245 pp.

Hodges, K.V. (2000) Tectonics of the Himalaya and southern Tibet from two decades perspectives. Geol. Soc. Amer. Bull., v. 112, pp. 324-350.

Hodges, K.V. , Parrish, R.R., Housh, T.B., Lux, D.R., Burchfiel, B.C., Royden, L.H. and Chen, Z. (1992) Simultaneous Miocene extension and shortening in the Himalayan orogeny. Science, v. 258, pp. 1466-1470.

Hollister, L.S. and Crawford, M.L. (1986) Melt enhanced deformation: a major tectonic process. Geology, v. 14(7), pp. 558-561.

Inger, S. and Harris, N.B.W. (1992) Tectonothermal evolution of the High Himalayan crystalline sequence, Langtang Valley, northern Nepal. J. Metam. Geol., v. 10, pp. 439-452.

Inger, S. and Harris, N. (1993) Geochemical constraints on leucogranite magmatism in the Langtang valley, Nepal Himalaya. J. Petrol., v. 34, pp. 345-368.

Jain, A. K., Kumar, D., Singh, S. Kumar, A. and Lal, N. (2000) Timing, quantification and tectonic modeling of Pliocene Quaternary movements in the NW Himalaya: evidences from fission track dating. Earth Planet. Sci. Lett., v. 179, pp. 437-451.

Jain, A. K., Singh, S. and Manickavasagam, RM. (in press) Himalayan Collision Tectonics, Bhagirathi Valley Garhwal. Gondwan Research Group Memoir No. 2002

Johannes, W. and Holtz, F. (1990) Formation and composition of H2O-undersaturated granitic melt. In: Asworth, J.R. and Brown, M. (eds) High temperature metamorphism and crustal anatexis, London; Unwin Hyman, pp. 87-104.

Jurewicz, W. and Watson, EB. (1984). Distribution of partial melt in felsic system : Importance of surface energy. Contrib. Min. Petrol., v. 85, pp. 125-129.

Jurewicz, W. and Watson, EB. (1985). The distribution of partial melt in granitic system : the application of liquid phase sintering theory. Geochim. Cosmochim. Acta, v. 49, pp. 1109-1121.

Kai, K. (1981) Rb-sr geochronology of the rocks of the Himalayas, Eastern Nepal. Part I. The metamorphic age of Himalayan Gneiss. Memoirs of the Faculty of Science, Kyoto University, Series of Geology and Mineralogy, v. 47, pp. 135-148.

Kwatra, S. K. Singh, S., Singh, V. P., Sharma, R. K., Rai, B. and Kishor, N. (1999) Geochemical and geochronological characteristics of the Early Palaeozoic Granitoids From Sutlej-Baspa Valley, Himachal Himalaya. In: Jain, A.K. and Manickavasagam, RM. (Eds.) Geodynamics of the NW-Himalaya, Gondwana Res. Group Mem. 6, pp. 145-158.

Le Fort, P. (1975) Himalayas: The collided range, Present knowledge of the continental arc. Amer. J. Sci., v. 275, pp.1-44.

Le Fort, P. (1981) Manaslu leucogranite: A collision signature of the Himalaya. A model for its genesis and emplacement. J. Geophys. Res., v. 86, pp. 10,545-10,568.

Le Fort, P. (1988) Granites in the tectonic evolution of Himalaya, Karakoram and southern Tibet. In: Tectonic evolution of the Himalayas and Tibet. Phil. Trans. R. Soc. London, v. 326, pp. 281-299.

Le Fort, P., Cuney, M., Deniel, C., Lanords, C.F., Sheppard, N.F., Upreti, B. N. and Vidal , P. (1987) Crustal generation of the Himalayan leucogranite. Tectonophysics, v. 134, pp. 39-57.

Le Preton, N. and Thompson, A.B. (1988) Fluid-absent (dehydration) melting of biotite in metapelites in the early stages of crustal anatexis. Contrib. Mineral. Petrol., v. 99, pp. 226-237.

McMahon, C.A. (1884) Microscopic structures of some

Himalayan granites and gneissose granites. Rec. Geol. Surv. India, v. 17, pp. 53-73.

Noble, S.R., and Searle, M.P. (1995) Age of crustal melting and leucogranite formation from U-Pb zircon and monazite dating in the Western Himalaya, Zanskar, India. Geology, v. 23 (12), pp. 1135-1138.

Odell, N.E. (1983) On the occurrence of granites in the Himalayan Mountains. In: Shams, F.A. (Ed.) Granites of Himalaya, Karakoram and Hindukush. pp. 1-10.

Pande, K. (1999) Present status of K-Ar and 40Ar-39Ar data from the Himalaya In: Jain, A.K. and Manickavasagam, R.M. (Eds.) Geodynamics of the NW-Himalaya. Gondwana Res. Group Mem. No. 6, pp. 237-244.

Pant, R. (1986) Petrochemistry and petrogenesis of the Gangotri granite and associated granitoids, Garhwal Himalaya. Unpubl. Ph. D. Thesis, Univ. Roorkee, India. 120 pp.

Pant, R. and Dave, V.K.S. (1992) Petrochemistry and petrogenesis of tourmaline-muscovite leucogranite of Gangotri, Uttarkashi district, Garhwal. Bull. Indian Geol. Assoc., v. 25(1-2), pp. 159-167.

Patino Douce, A.E. and Harris, N. (1998) Experimental constraints on Himalayan anatexis. J. Petrol., v. 39, pp. 904-911.

Pearce, J.A., Harris, N.B.W. and Tindle, A.G. (1984) Trace element discrimination diagram for the tectonic interpretation of granitic rocks. J. Petrol., v. 25, pp. 956-983.

Pognante, U. (1993) Different P-T-t paths and leucogranite occurrences along the High Himalayan Crystallines: Implications for subduction and collision along the northern Indian margin. Geodynamica Acta, v. 6(1), pp. 5-17.

Pognante, U., Genovese, G., Lombardo, B. and Rosetti, P. (1987) Preliminary data on the High Himalayan Crystallines along the Padam-Darcha traverse south eastern Zanskar, India. Rend. Soc. Ital. Miner. Petrol., v. 42, pp. 95-102.

Pichavant, M. and Montel, JM. (1988). Petrogenesis of a two mica ignimbrite suite : the Macusani volcanics, SE Peru. Trans. R. Soc. Edinburg (ES), v. 79, pp. 197-208.

Pichavant, M., Kontak, JD., Briqueu, L., Valencia herrara, J. and Clark, AH. (1988). The Macusani volcanics, SE Peru, II. Geochemistry and origin of a felsic peraluminous magma. Cont. Min. Petrol., v. 100, pp. 325-338.

Rathi, MS., Khanna, PP., Mukherjee, PK., and Saini, NK, (1996) Evaluation of REE determination in geological samples by inductively coupled plasma spectroscopy, Jour. Geol. Soc. India, v. 48, pp. 325-330.

Saini et al (2002)

Scaillet B., France-Lanord C. and Le Fort P. (1990) Badrinath-Gangotri plutons (Garhwal Himalaya): Petrological and geochemistry evidence for fractionation processes in a high Himalayan leucogranite. J. Volcan. Geotherm. Res., v. 44 (1/2), pp. 163-188.

Scaillet B., Pichavant, M. and Roux, J. (1995) Experimental crystallization of leucogranite magma. Jour. Petrol., v. 36, pp. 663-705.

Searle, M.P. (1991): Geology and Tectonics of the Karakoram Mountains. John Wiley & Sons, Chichester, 358 pp.

Searle, M.P and Fryer, B.J. (1986) Garnet, tourmaline, and muscovie-bearing leucogranites, gneisses and migmatites of the Higher Himalaya from Zanskar, Kulu, Lahoul and Kashmir In: Cowards, M.P. and Ries, A.C. (Eds.) Collision Tectonics. Geol. Soc. London Spec. Publ. No. 19, pp. 185-201.

Searle, M.P. and Rex, A.J. (1989) Thermal model of the Zanskar Himalaya. J. Metam. Geol., v. 7, pp. 124-134.

Searle, M.P., Cooper, D.J.W and Rex, A.J. (1988) Collision tectonics of the Ladakh-Zanskar Himalaya. Phil. Trans. R. Soc. London, v. A326, pp. 117-150.

Searle, M.P. Metcalfe, R.P., Rex, A.J. and Norry, M.J. (1993) Field relations, petrogenesis and emplacement of the Bhagirathi leucogranite, Garhwal Himalaya In: Treloar, P.J. and Searle, M.P. (Eds.) Himalayan Tectonics. Geol. Soc. London Spec. Publ. No. 74, pp. 429-444.

Searle, M.P., Parrish, R.R., Hodges, K.V., Hurford, A., Ayres, M.W. and Whitehouse, M.J. (1997) Shishma Pangma Leucogranite, South Tibetan Himalaya: field relations, geochemistry, age, origin and emplacement. J. Geol., v. 105, pp. 295-317.

Searle, M.P., Noble, S.R., Hurford, A.J. and Rex, D.C. (1999) Age of crustal melting, emplacement and exhumation history of the Shivling leucogranite, Garhwal Himalaya. Geol. Mag, v. 136 (5), pp. 513-525.

Seitz J.R. Tiwari, A.P. and Obradovich, K. (1976) A note on the absolute age of the tourmaline-granite, Arwa Valley Garhwal Himalaya-Geol. Surv. India Misc. Publ. v. 24 pp. 332-337.

Singh, R. P., 1986. Rb-Sr dating and Sr isotopic studies of some granites and gneisses of Kumaun and Garhwal Himalaya, U.P., India. Unpublished Ph.D. Thesis, Panjab University, Chandigarh.

Singh, S. (2001) Status of geochronological studies in Himalaya: a review. J. Indian Geophys. Union., v. 5 (1), pp. 57-72.

Sorkhabi, R.B., Stump, E., Foland, K.A. and Jain, A.K. (1996) Fission-track and 40Ar/39Ar evidence for episodic denudation of the Gangotri granites in the Garhwal Higher Himalaya, India. Tectonophysics, v. 260, pp. 187-199.

Sorkhabi, R.B., Stump, E., Foland, K.A. and Jain, A.K. (1999) Tectonic and cooling history of the Garhwal Higher Himalaya (Bhagirathi valley): constraining from thermochronological data In: Jain, A.K. and Manickavasagam, R.M. (Eds.) Geodynamics of the NW-Himalaya. Gondwana Res. Group Mem. No. 6, pp. 217-235.

Stern, C. R., Kligfield, R., Schelling, D., Virdi, N.S., Futa, K., Peterman, Z. E. and Amini, H. (1989) The Bhagirathi leucogranite of the High Himalaya (Garhwal, India): Age, petrogenesis and tectonic implications. Geol. Soc. Amer. Specl. Paper 232, pp. 33-45.

Vidal, Ph. (1978) Rb-Sr systematics in granites from Central Nepal (Manaslu): significance of the Oligocene age and high 87Sr/86Sr ratio in Himalayan Orogeny: comment. Geology, v. 6(4), pp. 196-200.

Wadia, D.N. (1928) The geology of the Poonch State, Kashmir and adjacent parts of the Panjab. Mem. Geol. Surv. India, v. 51, 233 pp.

Wadia, D.N. (1957) Geology of the India. McMillan & Co., London, 536pp.

Wendt, I. (1969) Derivation of the formula for a regression line based on a least square analysis. Internal. Rep. Bundesantalt Fur Bodenforschung, Hanover, West Germany.

Wickham, SM. (1987) The segregation and emplacement of granitic magma., Jour. Geol. Soc. London, v. 144, pp. 281-297.

Zen, E-AN (1986), aluminium enrichment in silicate melts by fractional crystallization : some mineralogic and petrographic constraints, Jour. Petrol., v. 27, pp. 1095-1117.